Building and Environment 47 (2012) 67–75

Contents lists available at ScienceDirect

Building and Environment

journal homepage: www.elsevier.com/locate/buildenv

An advanced numerical model for the assessment of airborne transmission of influenza in bus microenvironments

Shengwei Zhu [a,b,*], Jelena Srebric [b], John D. Spengler [a], Philip Demokritou [a,**]

[a] Department of Environmental Health, Harvard School of Public Health, Landmark Center, Room 421 West, 401 Park Dr., Boston, MA 02215, USA
[b] Department of Architectural Engineering, The Pennsylvania State University, 104 Engineering Unit A, University Park, PA 16802, USA

ARTICLE INFO

Article history:
Received 29 January 2011
Received in revised form
21 April 2011
Accepted 8 May 2011

Keywords:
Computational fluid dynamics (CFD)
Wells–Riley equation
Airborne infection transmission
Bus microenvironment
Mixing ventilation
Displacement ventilation

ABSTRACT

A CFD-based numerical model was integrated with the Wells–Riley equation to numerically assess the risk of airborne influenza infection in a popular means of public transportation, e.g. the bus microenvironment. Three mixing ventilation methods, which are widely used in current bus configurations, and an alternative displacement ventilation method were numerically assessed in terms of their ability to limit the risk of airborne influenza infection. Furthermore, both the non air-recirculation and air-recirculation with filtration ventilation modes were investigated in terms of the influenza infection probability. According to the simulation results, air-recirculation mode with high efficiency filtration was found to cause almost the same infection risk as non air-recirculation mode (100% outdoor air supply), which indicated a potential benefit of filtration in reducing the infection risk. Additionally, for the commonly used mixing ventilation methods, air distribution method, location of return/exhaust opening and seat arrangement affected the airborne transmission of influenza between passengers. The displacement ventilation method was found to be more effective in limiting the risk of airborne infection. Overall, the developed numerical model can provide insights into how the micro-environmental conditions affect airborne infection transmission in buses. This numerical model can assist in developing effective control strategies related to airborne transmitted diseases for other frequently used public transportation systems, such as trains and airplanes.

1. Introduction

In recent years, it became apparent that airborne transmitted diseases such as Tuberculosis (TB), Severe Acute Respiratory Syndrome (SARS), Avian Influenza and Swine Influenza (H1N1) are on a rise and may impose serious public health and financial burdens to our society. For example, the H1N1 pandemic spread rapidly around the world and caused as of July, 2010 over 18,366 deaths [1] with its full impact remained to be seen. Therefore, there is a need to further study and understand the transmission of airborne infectious diseases in indoor environments, especially in microenvironments with high occupant density such as the public transportation means (e.g. buses, trains, airplanes).

Many studies of airborne transmission of respiratory infectious diseases focused on various indoor microenvironments, such as hospital ward [2] and aircraft cabin [3–6], and primarily emphasized the mechanisms of airborne transmission and the development of efficient infection-control strategies. Bus systems are a popular mean of public transportation around the world [7]. A number of studies on bus microenvironments have reported serious indoor environment quality (IEQ) problems with many indoor pollutants at higher concentration levels than outdoors. A Hong Kong-based field study found that CO_2 concentration levels could be up to 10 times higher than outdoor concentrations under overcrowded conditions in the bus system [7]. Similarly, a field study in Boston, MA (USA) found that CO_2 concentration levels were elevated and greatly affected by occupancy rates [8], which is an indication of insufficient ventilation in the bus microenvironments. The insufficient ventilation and overcrowded conditions in the bus microenvironments, which unfortunately are the norm in many cities around the world, may increase the risk of airborne transmission of various infectious diseases. Therefore, alternate control strategies need to be developed and employed in order to protect the public from airborne transmitted infectious diseases.

* Corresponding author. Department of Architectural Engineering, The Pennsylvania State University, 104 Engineering Unit A, University Park, PA 16802, USA. Tel.: +1 814 863 8313; fax: +1 814 863 4789.
** Corresponding author. Tel.: +1 617 384 8847; fax: +1 617 384 8819.
E-mail addresses: SZHU@hsph.harvard.edu (S. Zhu), PDEMOKRI@hsph.harvard.edu (P. Demokritou).

0360-1323/$ – see front matter © 2011 Elsevier Ltd. All rights reserved.
doi:10.1016/j.buildenv.2011.05.003

Computational Fluid Dynamics (CFD) modeling has been used successfully to study the spatial and temporal distributions of temperature, velocity and contaminants in various micro-environmental settings including aircraft cabins [4,5,9], trucks [10], cars [11,12], and buses [8]. CFD was also proved to be a powerful tool to study the fate and transport of exhaled bio-aerosols [5,13,14], which are technically difficult to measure in real world conditions.

Here, a recently developed and validated CFD model [8] for the bus microenvironment was integrated with the Wells–Riley equation [15] in order to numerically assess the risk of airborne transmission of influenza in bus microenvironments. Three mixing ventilation systems commonly used in buses, were studied in terms of their ability to minimize the risk of airborne infection. In addition, as an alternate ventilation method, displacement ventilation was also investigated. Furthermore, both the non air-recirculation and air-recirculation integrated with filtration ventilation methods were considered in this study as an alternative control strategy.

2. Method

2.1. An integrated numerical model to predict infection probability for airborne diseases

The probability of indoor airborne transmission of an infectious agent can be estimated from the Wells–Riley equation [15,16] as follows:

$$P = \frac{C}{S} = 1 - e^{-Iqpt/Q} \tag{1}$$

Where, P is the probability of infection for a susceptible person, C is the number of infection cases, S is the number of susceptible people, I is the number of infectors, p is the breathing rate of a susceptible person ($m^3\ s^{-1}$), q is the quantum generation rate by an infector (quanta$\cdot s^{-1}$), t is the total exposure time (s), and Q is the outdoor air supply rate ($m^3\ s^{-1}$).

Eq. (1) was derived based on the following assumptions: 1) well-mixed and steady state air conditions; 2) no biologic decay of infectious virus; and 3) no infectious particles elimination due to filtration and/or deposition.

The airborne viruses can be assumed to be attached to exhaled particles, and therefore the distribution of airborne viruses is similar to that of the airborne particles [2]. Based on the drift-flux particle model [17], the transport of airborne infectious particles can be calculated using the following governing equation:

$$\frac{\partial(\rho N)}{\partial t} + \nabla\cdot(\rho(\vec{V} + \vec{V}_s)N) = \nabla\cdot(\Gamma\nabla N) - k\rho N + S \tag{2}$$

Where, ρ is the density of air (kg m^{-3}); N is the concentration of quanta, e.g. the infectious particles with viruses attached on their surfaces (quanta$\cdot m^{-3}$); $\vec{V}$ is the velocity vector of air (m s^{-1}); $\vec{V}_s$ is the settling velocity vector of particles (m s^{-1}) ($\vec{V}_s$ can be calculated using the density and particle size with Stokes law); Γ is the diffusion coefficient of the particles (kg $m^2\ s^{-1}$); k is the constant decay rate of the airborne organisms in the air (s^{-1}); S is the source term. It is also worth pointing out that for the model development, while humidity levels and temperatures may affect droplet evaporation and change droplet size, droplet evaporation was neglected and 5 μm droplet nuclei size was selected as the size of interest for influenza [2] and used in the simulations. The decay rate k of influenza viruses was assumed to be zero.

The deposition of particles J (quanta$\cdot m^{-2}\ s^{-1}$) at the floor and other upward surfaces of seats and walls can be estimated as follows [2,18,19]:

$$J = -v_d N_\infty \tag{3}$$

Where v_d is the deposition velocity (m s^{-1}) and N_∞ is the concentration of quanta (particles) in the air near the surfaces (quanta$\cdot m^{-3}$). In the model, the particle size was assumed to be 5 μm, for which the settling velocity is about 7.5×10^{-4} m/s. The deposition velocity (v_d) onto the floor and vertical smooth surfaces in the indoor environment is very close to the settling velocity for 5 μm diameter particles [2,18,19].

If the airflow vectors are known, the spatial distribution of quantum concentration can be estimated numerically from Eq. (2). In this study, the authors' recently developed and validated CFD model for the bus microenvironment was used to calculate the velocity, temperature and contaminant distributions in the bus [8]. Consequently, the infection risk P for a passenger, can be estimated from Eq. (4) as follows:

$$P = 1 - e^{-pNt} \tag{4}$$

In a well-mixed air environment, N will be equal to Iq/Q as shown in Eq. (1).

2.2. Simulation scenarios

A total of four ventilation scenarios were used in this study. Each ventilation scenario and its conditions are summarized in Fig. 1 and Table 1. In Scenario #1, the original bus ventilation system was simulated (Fig. 2). The air was supplied through linear air diffusers with a total area of 0.21 m^2 and the air return/exhaust opening was located in the middle of the ceiling close to the middle doors. Scenario #2 had the same linear air diffuser as Scenario #1 with the air return/exhaust opening located in the center of the back wall. In Scenario #3, the linear air diffusers were replaced by eight round air diffusers with a total area of 0.16 m^2. Each round diffuser had a diameter of 16 cm and supplied air downwards. The location of the return/exhaust opening was same as in Scenario #1. Finally, in Scenario #4, the displacement ventilation method was employed instead of the mixing ventilation method used in other scenarios. The linear air supply openings were located 5 cm above the floor (Fig. 1)(d). They were 20 cm in height with a total area of 2.34 m^2. Air was supplied upward with an angle of 10° from the horizontal direction. Two linear air return/exhaust openings were located at each side of the ceiling with a total area of 1.43 m^2.

Furthermore, for each ventilation scenario described above, both the non air-recirculation and air-recirculation with filtration modes were considered. For the air-recirculation mode, the air recirculation rate was set to be 25% and the filter efficiency for 5 um size particles was assumed to be 75%. The total air supply rate was the same in each scenario with a value of 0.54 $m^3\ s^{-1}$ based on our field measurements [8]. It is also worth to note that for all scenarios the doors and windows were considered closed, thus air infiltration was assumed to be zero.

In all the scenarios, an occupancy rate of 26 seated people and 4 standing people was assumed (Fig. 3). Therefore, for each scenario, a total of 30 simulations were conducted in order to estimate the infection probability for each person. In each simulation, one of the passengers was assumed to be the influenza infector doing continuous exhalation (continuous source), with the remaining passengers being the susceptible ones and doing continuous inhalation simultaneously. The continuous inhalation and exhalation assumptions have been validated [20,21], and applied to a number of studies including both numerical [22–24] and experimental methods [24,25].

According to our previous field measurement study [8], the passengers rarely moved in the bus unless they were getting on/off

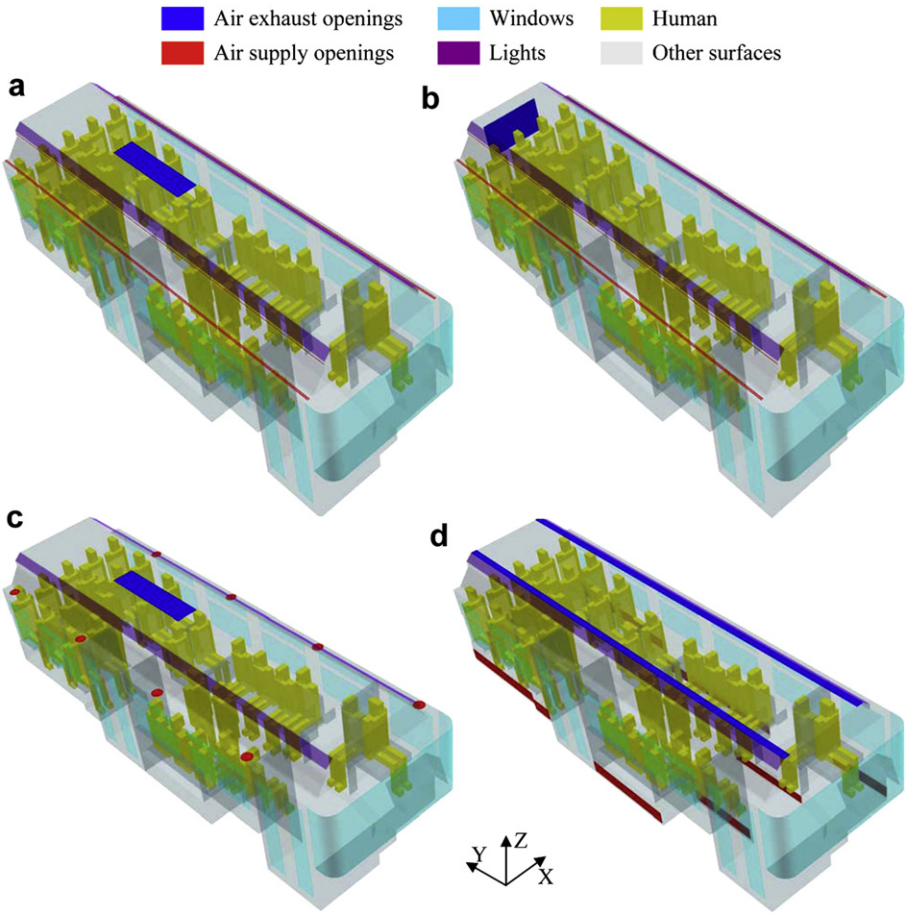

Fig. 1. Bus cabins used in simulations: (a) bus cabin in Scenario #1; (b) bus cabin in Scenario #2; (c) bus cabin in Scenario # 3; (d) bus cabin in Scenario #4.

the bus. Moreover, the change of CO_2 concentration levels was small even when the doors were opened to allow entrance/exit of passengers, if there were no or little change in the total occupancy load. This minimal and localized effect of outdoor air inflow can be attributed to the great air exchange rate of 57.6 ACH (no air recirculation), which shows the capability to restore the bus microenvironment soon after the interruptions of the bus microenvironmental conditions. Therefore, the influence of any environmental changes that might be caused by the events, such as movement of the passengers and the door operation, were neglected by assuming a steady state.

Table 1
Boundary Conditions in CFD simulations.

Air supply opening	Airflow rate: 0.54 $m^3\ s^{-1}$; Temp: 20.2 °C; Vel: 2.54 $m{\cdot}s^{-1}$ in Scenario #1 and 2, 3.37 $m{\cdot}s^{-1}$ in Scenario #3, 0.23 $m{\cdot}s^{-1}$ in Scenario #4; Turb. intensity: 2.5%; Turb. scale: 0.005 m
Air exhaust opening	Free-slip
Mouth openings	Vel.: 1.87 $m{\cdot}s^{-1}$ for driver, 1.07 $m{\cdot}s^{-1}$ for other people; Temp.: 20.2 °C when inhalation, 34 °C when exhalation; Turb. intensity: 10%; Turb. scale: 0.0075 m
Body surfaces	No-slip; Temp.: obtained in experiment as described in the text
Lights	No-slip; Temp.: 25.0 °C
Floor	No-slip; Temp.: 15.5 °C (in front compartment), 19.8 °C (in rear compartment)
Front windshield	No-slip; Temp.: 31.8 °C
Windows in front door	No-slip; Temp.: 12.3 °C
Windows in middle door	No-slip; Temp.: 14.0 °C
Windows on the side of doors	No-slip; Temp.: 12.3 °C (in front compartment), 14.6 °C (in rear compartment)
Windows on the side of driver	No-slip; Temperature: 21.0 °C
Other walls	No-slip; adiabatic conditions

2.3. Boundary conditions in CFD simulations

2.3.1. Human occupancy

The seat arrangement and location for the driver and the 29 passengers are shown in Fig. 3. Each human body was simplified and made up of 13 rectangular parts: face, head, body (including neck), as well as left and right arm, hand, thigh, leg and foot. Arms and hands were made to be connected and integrated with the body. Height for all passengers was assumed to be 170 cm. The people were also assumed to wear clothes for autumn conditions, with only faces and hands exposed in the air. Heads were considered to be covered with hair. The body surface temperatures used in the simulations were measured by a thermal infrared camera (Maker: FLIR; Model: B60) in a subject experiment conducted in a climate chamber with similar air temperature and velocity distributions as in Scenario #1. Furthermore, the subject in these experiments had slightly heavy clothes for late autumn. Based on the experiments, for the seated people, the surface temperature was 34 °C at face and hands, 30 °C at thighs and feet, 28 °C at head, 24 °C at trunk and arms and 23 °C at legs; for the standing people, the surface temperature was different at face (33.5 °C), thighs (24 °C) and legs (24 °C). In addition, the mouth was modeled as a rectangular opening (L2cm × H1.5 cm). The driver was assumed

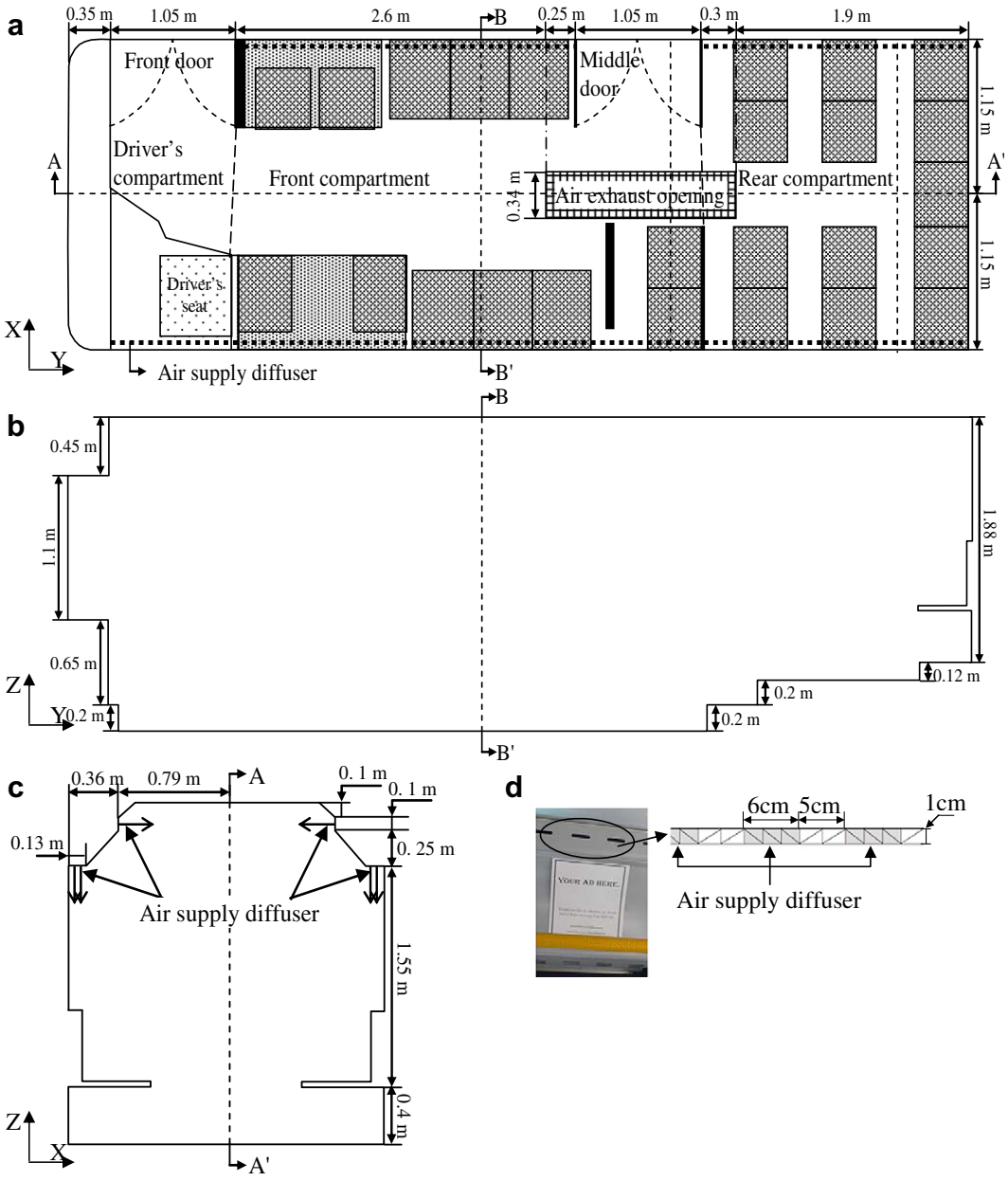

Fig. 2. Geometrical characteristics of the bus cabin in Scenario #1: (a) top view; (b) cross section A–A′; (c) cross section B–B′; (d) real shape and CFD model of linear air supply diffuser.

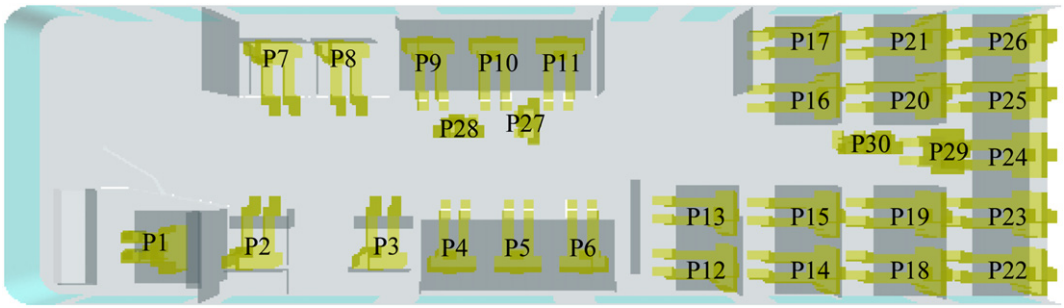

Fig. 3. Seat arrangement in buses (P1: driver, P2-P30: passengers).

to have a metabolic rate of 1.8 met and breathe at a rate of 14 l/min; all passengers were assumed to be in a relatively quiet state with a metabolic rate of 1.0 met and breathe at a rate of 8 l/min [26]. In the simulations, air was inhaled or exhaled from the mouth with only a horizontal direction.

2.3.2. Bus cabin geometry

The internal bus cabin geometric characteristics used in all our simulation scenarios were made similar to a Daimler-Chrysler SLF 200 as shown in Fig. 2. The surface temperatures of floor, windows and lights, as well as the turbulence intensity and airflow rate at the air supply openings were measured in a field experiment and previously reported in the literature [8] and are summarized in Table 1. The rest of wall surfaces were assumed adiabatic.

2.4. Numerical procedure

For all scenarios, the internal bus space was made up of approximately 120 million tetrahedral spatial cells and 200,000 triangular surface meshes. Moreover, approximately 2700 surface meshes were used for seated, and 2936 for standing human bodies. The grid systems were created using Gridgen V15.10 at a growth rate of 1.1. The grid quality was ensured with EquiAngle Skewness to be less than 0.84 for all meshes.

The commercial CFD software, Star-CD V4.08, was used to solve the governing equations together with the standard k-ϵ model and implicit SIMPLE algorithm [27]. The finite volume method with the first-order upwind scheme was adopted for discretizing the governing equations. Solar and long wave radiation was not considered in the simulations. Moreover, the standard wall function [28] was used for the near wall boundary layer. After obtaining the flow field, a generic scalar was used to calculate the transport of influenza quantum with Eq. (2). The generation rate of infection quanta of influenza was assumed to be 67 quanta$\cdot h^{-1}$ at the mouth of the infector [29]. The scalar simulations provided the concentration of influenza quantum at the mouth opening of each susceptible person. Finally, Eq. (4) was used to calculate the influenza infection risk for each susceptible person using the calculated quantum concentration at his/her mouth. Moreover, the exposure time was set to 10 min according to the period of a typical bus route in the previous experimental study [8].

3. Results

3.1. Airflow streamlines in the bus for each ventilation scenario

Fig. 4–7 indicate the airflow streamlines of supplied and exhaled air from a number of infected passengers for scenarios #1–4, respectively. In each scenario, the infected passenger was seated in a specific location (passengers P8, P12, P21, P27 and P30 as numbered in Fig. 3). The airflow streamlines are colored by air velocity magnitude.

It is obvious that for mixing ventilation methods (Scenarios #1, 2 and 3), the location of the infected person in combination with the air distribution method and location of the air return/exhaust opening defined the streamlines of exhaled air in the cabin. Obviously, the passengers located between the infected person and the air return/exhaust opening would have greater risk for infection. For Scenario #4 with displacement ventilation, it is obvious that air was purged quite nicely from the cabin by supplying the air at the floor level and exhausting it from the ceiling. Therefore, the airflow streamlines from the infected person to the exhaust opening was very limited and only people in the immediate vicinity of the infector were exposed and at risk.

3.2. Airborne infection probability for influenza virus

3.2.1. Air-recirculation versus non air-recirculation modes

According to the simulation results, when the ventilation system was operated with 25% air-recirculation and coupled with a 75% efficiency filtration system, regardless of ventilation scenario and/or infector's location, the probability for a passenger to be infected by anyone else in the bus increased by only 0.05%, compared to the non air-recirculation mode. The driver was found to have a slightly higher probability to get infected (around 0.09%) compared to the non air-recirculation mode, which was attributed to the slightly higher breath rate.

3.2.2. Effect of ventilation methods

Fig. 8 (a), (b), (c), and (d) show the probabilities for the four randomly selected seated passengers (P5, P8, P12 and P21) to get infected by the driver and the rest of the passengers for each ventilation scenario. It is clear that in Scenario #4 with

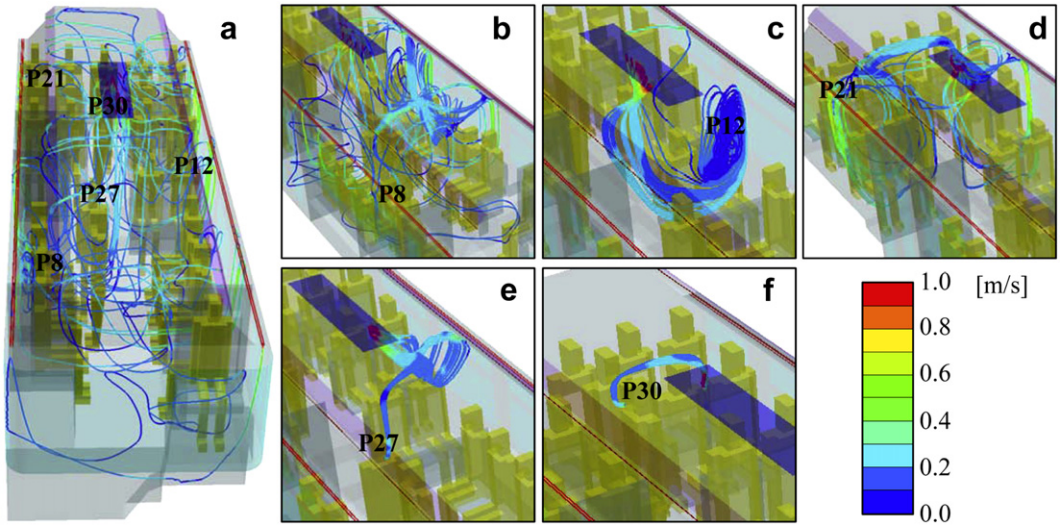

Fig. 4. Airflow streamlines of supplied and exhaled airflows in Scenario #1: (a) supplied airflow; (b) exhaled airflow of P8; (c) exhaled airflow of P12; (d) exhaled airflow of P21; (e) exhaled airflow of P27; (f) exhaled airflow of P30.

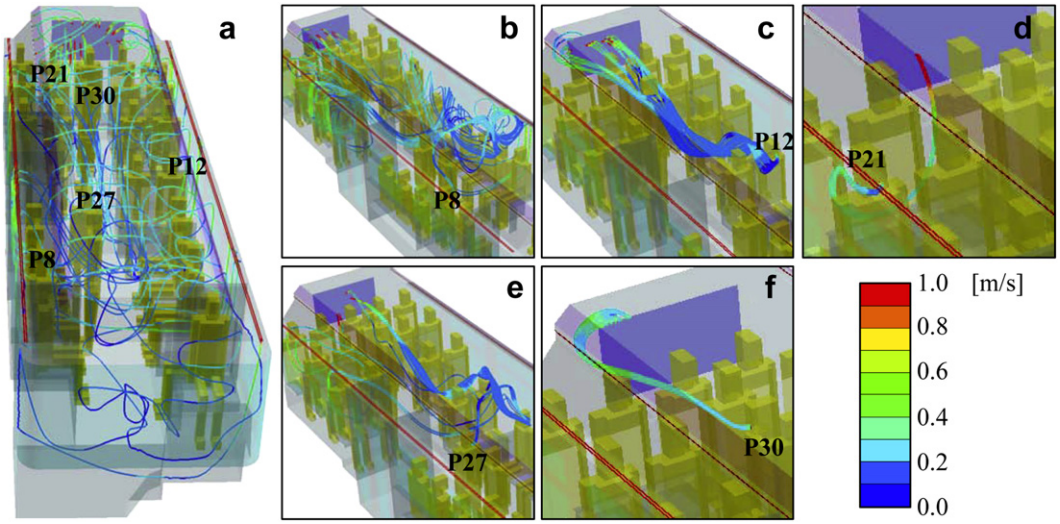

Fig. 5. Airflow streamlines of supplied and exhaled airflows in Scenario #2: (a) supplied airflow; (b) exhaled airflow of P8; (c) exhaled airflow of P12; (d) exhaled airflow of P21; (e) exhaled airflow of P27; (f) exhaled airflow of P30.

displacement ventilation method, the location of person-source did not affect the risk of airborne infection for the rest of the passengers, with the risk to be very low (around 0.05%). In all other ventilation scenarios, the probability of an airborne infection for these four passengers varied from 0.05% to 10.1%. It is worth pointing out that if the susceptible passenger is seated between the infector and the air return/exhaust opening, then the risk increased.

Fig. 9(a), (b), (c), and (d) show the probabilities for each of the standing passengers (P27, P28, P29 and P30) to get infected by any other passenger in the bus. Similarly to the seated passengers described above, the displacement ventilation method (Scenario #4) was found to be a better control strategy in terms of limiting the risk of airborne infection for the standing passengers. In all other ventilation scenarios, the "air mixing" influenced significantly the risk for airborne infection. In Scenario #3, P9's exhaled infectious particles caused an infection probability as high as 22% for passenger P27. Similarly, P8's exhaled infectious particles caused a greater infection probability of 27.2% for passenger P28. These findings indicate that the standing passengers in the front compartment have higher risks of getting infected due to the fact that they were in the highly turbulent mixing zone of the cabin. Furthermore, the location of the air return/exhaust opening influenced the risk of airborne infection for the passengers standing in the rear compartment.

4. Discussion

Based on the aforementioned simulation results, it becomes apparent that the closer to the exhaust opening the infected person is, the shorter the pathway of the exhaled air in the cabin is, which results in smaller infection risks for the passengers in the bus. This is a quite important finding in terms of the ventilation method employed by the bus manufacturers. Most bus manufacturers use only a single air return/exhaust opening located either in the middle of the ceiling or the back wall (scenarios #1, 2 and 3). It is quite obvious that these methods are not the most efficient methods in terms of minimizing the contact of the people from emitted bio-aerosols. This is in line with the results from the

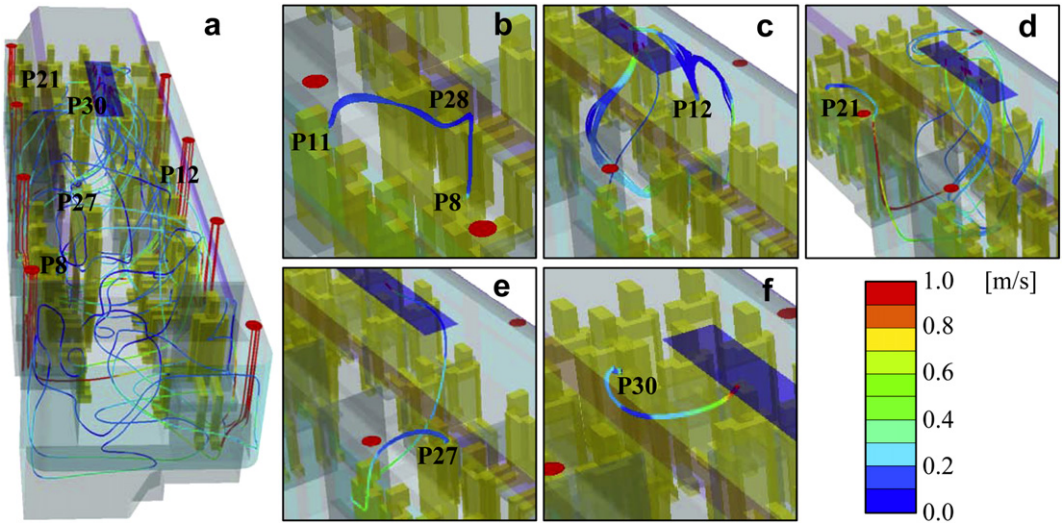

Fig. 6. Airflow streamlines of supplied and exhaled airflows in Scenario #3: (a) supplied airflow; (b) exhaled airflow of P8; (c) exhaled airflow of P12; (d) exhaled airflow of P21; (e) exhaled airflow of P27; (f) exhaled airflow of P30.

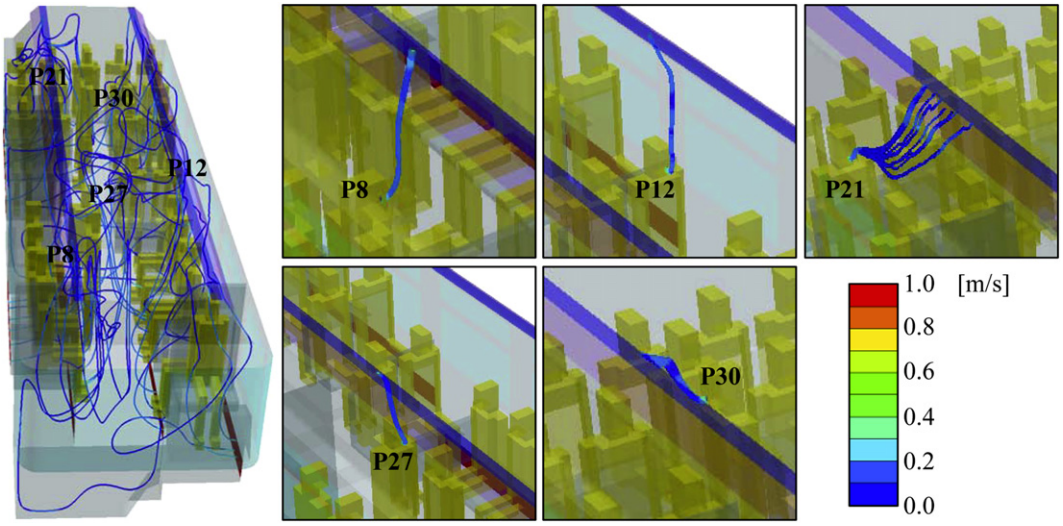

Fig. 7. Airflow streamlines of supplied and exhaled airflows in Scenario #4: (a) supplied airflow; (b) exhaled airflow of P8; (c) exhaled airflow of P12; (d) exhaled airflow of P21; (e) exhaled airflow of P27; (f) exhaled airflow of P30.

previous field studies [7,8] which linked the lack of proper ventilation in bus microenvironments as well as the ventilation methods to increased risks for airborne transmission of infectious diseases. On the contrary, the displacement ventilation method (Scenario #4) minimizes the air mixing in the cabin and reduces the contact of the exhaled bio-aerosols with the rest of the passengers, resulting in lower infection risks for the passengers.

The 25% air recirculation mode combined with a 75% efficiency filtration system results in almost the same infection probability with the non air-recirculation mode (100% outdoor air supply). The air recirculation mode is justifiably adopted in practice to reduce the energy consumption for maintaining thermal comfort in the buses. However, the air recirculation is also considered to be a factor in the airborne transmission of diseases. This finding supports the hypothesis that installing filtration systems in current buses that use air recirculation may be an effective control strategy to minimizing the risk of airborne infection induced by air recirculation.

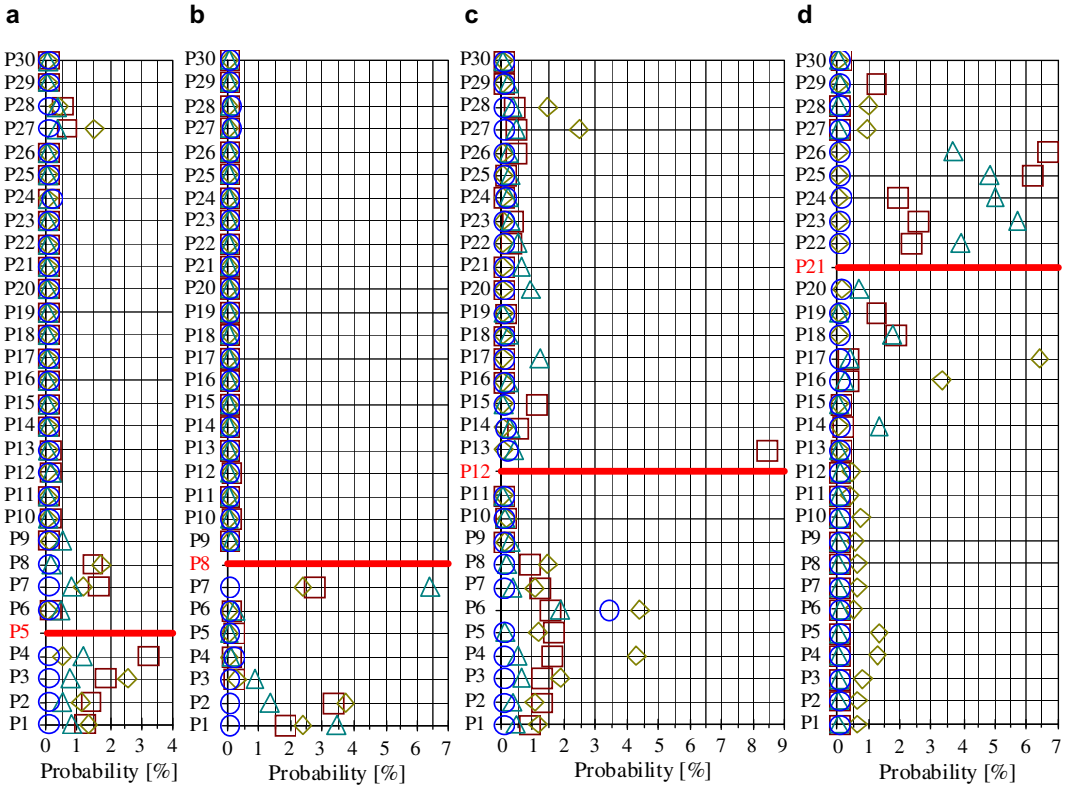

Fig. 8. Probabilities of airborne influenza infection by any other passenger for four seated passengers after a 10-min exposure: (a) P5 is the susceptible person; (b) P8 is the susceptible person; (c) P12 is the susceptible person; (d) P21 is the susceptible person.

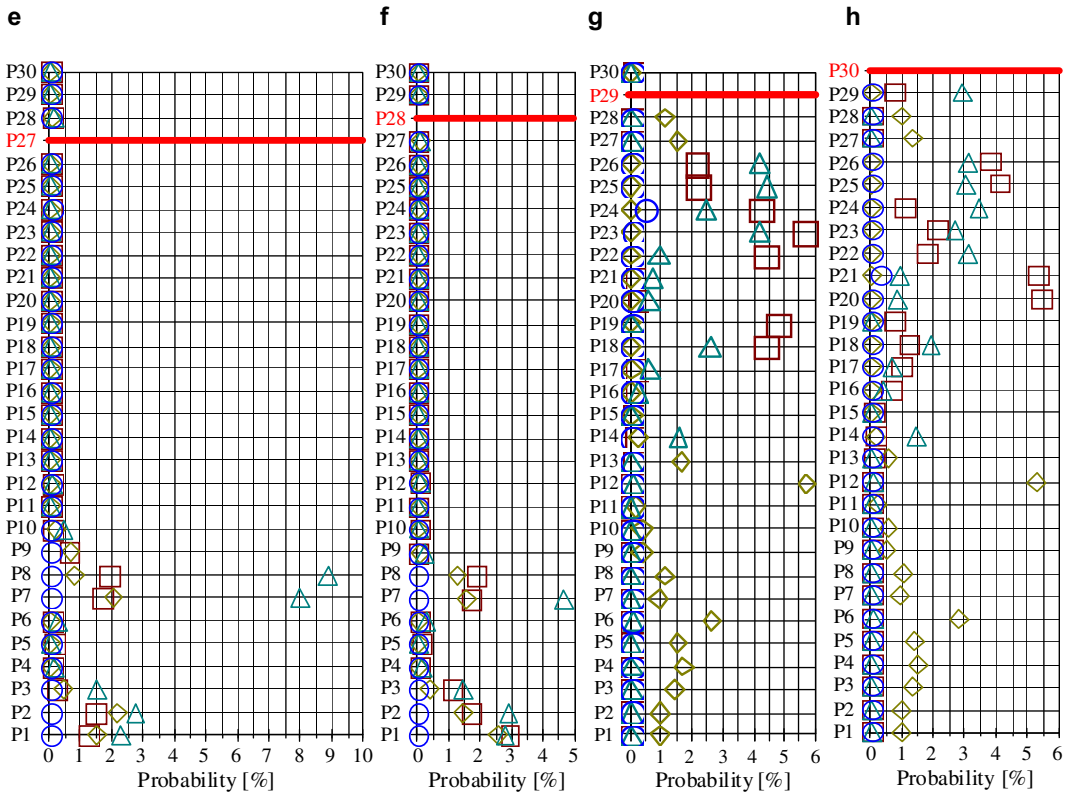

Fig. 9. Probabilities of airborne influenza infection by any other passenger for four standing passengers after a 10-min exposure: (a) P27 is the susceptible person; (b) P28 is the susceptible person; (c) P29 is the susceptible person; (d) P30 is the susceptible person.

5. Conclusions

The CFD-based numerical model integrated with the Wells–Riley equation is a powerful tool that can be used to assess the link between micro-environmental conditions and airborne transmission of infectious diseases. These micro-environmental conditions result from the air distribution method, location of air return/exhaust opening, air recirculation and filtration. The developed numerical model was successfully applied to a popular mean of public transportation, to study the risk of airborne infection of influenza and develop effective control strategies for this unique bus microenvironment. The developed model can help public health professionals to further develop effective strategies in terms of controlling airborne transmitted diseases in many other microenvironments such as trains and airplanes. It becomes apparent from the results that the current bus ventilation methods are problematic in terms of their ability to limit the risk of an airborne infection, so alternate ventilation strategies such as displacement ventilation method may be implemented by the manufacturers. Another control strategy that may help to minimize the exposure of the public to airborne infectious viruses while using public transportation systems is the use of filtration systems. We plan to further use the developed numerical model to investigate other important public transportation microenvironments and come up with effective control strategies that can protect the public from airborne transmission of infectious diseases.

Acknowledgment

This study was supported by the Environmental Fellows Program at Harvard University Center for the Environment. The authors would like to express their gratitude to Harvard University Transportation Services for granting access to their buses for this study. Also, we are very grateful to Dr. Kato Shinsuke from Institute of Industrial Science, The University of Tokyo that shared the CFD resources with us.

References

[1] WHO. World Health Organization, http://www.who.int/csr/don/2010_07_23a/en/index.html; 2010.
[2] Qian H, Li YG, Nielsen PV, Huang X. Spatial distribution of infection risk of SARS transmission in a hospital ward. Building and Environment 2009;44(8):1651–8.
[3] Ko G, Thompson KM, Nardell EA. Estimation of tuberculosis risk on a commercial airliner. Risk Analysis 2004;24(2):370–87.
[4] Lin CH, Horstman RH, Ahlers MF, Sedgwick IM, Dunn KH, Topmiller JL, et al. Numerical simulation of airflow and airborne pathogen transport in aircraft cabins-Part I: numerical simulation of the flow field. ASHRAE Transactions 2005;111(1):755–63.
[5] Lin CH, Horstman RH, Ahlers MF, Sedgwick IM, Dunn KH, Topmiller JL, et al. Numerical simulation of airflow and airborne pathogen transport in aircraft cabins-Part II: numerical simulation of airborne pathogen transport. ASHRAE Transactions 2005;111(1):764–8.
[6] Sze-To GN, Wan MP, Chao CYH, Fang L, Melikov AK. Experimental study of dispersion and deposition of expiratory aerosols in aircraft cabins and impact on infectious disease transmission. Aerosol Science and Technology 2009;43(5):466–85.
[7] Chan AT. Commuter exposure and indoor-outdoor relationships of carbon oxides in buses in Hong Kong. Atmospheric Environment 2003;37(27):3809–15.
[8] Zhu SW, Philip D, Spengler JD. Experimental and numerical investigation of micro-environmental conditions in public transportation buses. Building and Environment 2010;45(10):2077–88.
[9] Zhang T, Chen Q. Novel air distribution systems for commercial aircraft cabins. Building and Environment 2007;42(4):1675–84.
[10] S.Tanabe. Prediction of indoor thermal comfort in vehicle by a numerical thermoregulation model and CFD. In: Proceedings of the 9th International Conference on air distribution in room; 2004.
[11] A.Alexandrov,V.Kudriavtsev, M.Reggio. Analysis of flow patterns and heat transfer in generic passenger car mini-environment. In: Proceedings of the 9th Annual Conference of the CFD Society of Canada; 2001.
[12] Nagano H, Zhu SW, Ozeki Y, Kato S, Matsunaga K, Kataoka T. Ventilation characteristics of modeled compact car (Part 2) Estimation of local ventilation

efficiency and inhaled air quality. SAE International Journal of Passenger Cars-Mechanical Systems 2008;1(1):623–30.
[13] Zhu SW, Kato S, Yang JH. Study on transport characteristics of saliva droplets produced by coughing in a calm indoor environment. Building and Environment 2006;41(12):1691–702.
[14] Mui KW, Wong LT, Wu CL, Lai ACK. Numerical modeling of exhaled droplet nuclei dispersion and mixing in indoor environments. Journal of Hazardous Materials 2009;167(1–3):736–44.
[15] Riley EC, Murphy G, Riley RL. Airborne spread of measles in a suburban elementary school. American Journal of Epidemiology 1978;107(5):421–32.
[16] Wells WF. Airborne contagion and air hygiene: an ecological study of droplet infection. Cambridge, MA: Harvard University Press; 1955.
[17] Holmberg S, Li YG. Modelling of the indoor environment-Particle dispersion and deposition. Indoor Air 1998;18(2):113–22.
[18] Lai ACK, Nazaroff EE. Modeling indoor particle deposition from turbulent flow onto smooth surfaces. Journal of Aerosol Science 2000;31(4):463–76.
[19] Gao NP, Niu JL. Modeling particle dispersion and deposition in indoor environments. Atmospheric Environment 2007;41(18):3862–76.
[20] Murakami S. Analysis and design of micro-climate around the human body with respiration by CFD. Indoor Air 2004;14(7):144–56.
[21] Zhu SW, Kato S, Murakami S, Hayashi T. Study on inhalation region by means of CFD analysis and experiment. Building and Environment 2005;40(10):1329–36.
[22] Zhu SW, Hayashi T, Kato S, Murakami S. Investigation of flow field in human's respiration area in a calm environment by visualization experiment and numerical analysis. Journal of Environmental Engineering 2004;583:37–42 (In Japanese).
[23] Hayashi T, Kato S, Murakami S, Zhu SW, Yang JH. CFD analysis on contribution ratio of pollution source to breathing air quality in a stagnant room. Journal of Environmental Engineering 2006;603:41–5 (In Japanese).
[24] Qian H, Li YG, Nielsen PV, Hyldgaard CE. Dispersion of exhalation pollutants in a two-bed hospital ward with a downward ventilation system. Building and Environment 2008;43(3):344–54.
[25] Yin Y, Gupta JK, Zhang X, Liu J, Chen Q. Distributions of respiratory contaminants from a patient with different postures and exhaling modes in a single-bed inpatient room. Building and. Environment 2011;46(1):75–81.
[26] Nishi Y, Miyazaka A, Horikosi T, Ishii A, Hanzawa H, Tsuchikawa T, et al. Human and thermal environment. In: Mechanism of comfortable thermal environment. Japan: Maruzen; 1997. 2005.
[27] Patankar SV. Calculation of the flow field. In: Numerical heat transfer and fluid flow. New York: Hemisphere Publishing Corp; 1980.
[28] Launder BE, Spalding DB. The numerical computation of turbulent flows. Computer Methods in Applied Mechanics and Engineering 1974;3(2):269–89.
[29] Liao CM, Chang CF, Liang HM. A probabilistic transmission dynamic model to assess indoor airborne infection risks. Risk Analysis 2005;25(5):1097–107.